Infrared stimulated luminescence and phosphorescence spectra of irradiated feldspars

2003 J. Phys.: Condens. Matter 15 8029

(http://iopscience.iop.org/0953-8984/15/46/018)

INSTITUTE OF PHYSICS PUBLISHING JOURNAL OF PHYSICS: CONDENSED MATTER

J. Phys.: Condens. Matter **15** (2003) 8029–8048 PII: S0953-8984(03)66018-2

Infrared stimulated luminescence and phosphorescence spectra of irradiated feldspars

Marc René Baril[1] **and D J Huntley**

Department of Physics, Simon Fraser University, 8888 University Drive, Burnaby, BC, V5A 1S6, Canada

E-mail: marcrene@sfu.ca

Received 4 July 2003
Published 7 November 2003
Online at stacks.iop.org/JPhysCM/15/8029

Abstract

A new high-sensitivity wide-bandwidth 1.25–5.5 eV (225–1000 nm) spectrometer has been constructed to measure luminescence emission spectra of minerals that are of interest for optical dating. Spectra of emission resulting from 1.43 eV (IR) excitation after γ-irradiation are reported for 13 cut rock feldspars and 20 feldspar separates. Also reported are phosphorescence spectra following γ-irradiation, and after 1.4 eV excitation. The main differences between the infrared stimulated luminescence spectra and the phosphorescence is the almost complete absence of the violet, 3.1 eV, and yellow–green, 2.2 eV, bands in the phosphorescence, and the presence of a green emission band centred at 2.7 eV in the phosphorescence following γ-irradiation (but absent in the phosphorescence following 1.4 eV excitation). The red, 1.7 eV, band is present in all the phosphorescence spectra but is not always seen during 1.4 eV excitation. A band at $\sim$1.3 eV is dominant in both types of phosphorescence spectra. This dependence of the luminescence spectrum on the mode of excitation suggests a strong correlation between certain traps and luminescence centres. Models involving recombination via a 'conduction band' in the traditional sense cannot account for these observations.

1. Introduction

Optical dating is a geological tool that relies on the optically stimulated luminescence of naturally irradiated minerals to determine the last exposure of minerals to sunlight (Aitken 1998). The luminescence arises from electrons that are optically excited out of traps in which they are thermally stable, recombining at other defects in the mineral. The use of potassium feldspars in dating has been popular due to the brightness of their violet infrared stimulated luminescence, the high dose of ionizing radiation necessary to produce saturation of their

[1] Author to whom any correspondence should be addressed.

luminescence and their abundance in sediments. The excitation of the optically stimulated luminescence in feldspars has a resonance in the infrared at 1.44 eV. This indicates that the trapped electrons are optically excited to a metastable level of the trap before proceeding to a recombination centre. The identity of the trap defect is unknown, and few of the luminescence centres have been conclusively identified (see Krbetschek *et al* (1997) for a review).

The traditional view of luminescence spectra is that they only provide information about the luminescence centres and not the traps from which the electrons are excited. This statement relies on the conventional assumption that, after excitation, electrons are in the conduction band and free to move throughout the crystal. This assumption is supported by the similarity of the 1.4 eV excited and high-temperature thermoluminescence (TL) spectra, in particular the 3.1 eV (violet) and 2.2 eV (yellow–green) emission bands (Huntley *et al* 1991). The present work provides contrary evidence.

Spectral information was obtained for a wide variety of detrital and cut rock feldspar samples of known composition. A new spectrometer allowed measurements of 1.4 eV excited luminescence to within 0.25 eV of the excitation. In addition, the phosphorescence immediately following γ-irradiation and the phosphorescence following illumination of an irradiated sample by 1.43 eV excitation photons were measured. The three spectra are found to have marked differences.

2. The spectrometer

Several methods have been used to measure the spectral emission of the dim and transient, thermally and optically excited luminescence in minerals; these are summarized in table 1. The highest throughput is obtained using a Fourier transform spectrometer. Such a system was developed by Prescott *et al* (1988) for measuring TL spectra. The maximum étendue of Prescott's instrument is approximately 180π mm^2, with a resolution of 20 nm. This assumes a sample of diameter equivalent to the limiting aperture ($\sim$5 cm). In practice the sample is much smaller than this (1 cm in diameter), so the effective étendue is closer to $\sim 7\pi$ mm^2.

Oczkowski (1992) employed a variable interference filter and a multi-slit Hadamard encoding mask to produce a spectrometer with a throughput of $\sim 4\pi$ mm^2 (assuming a 1 cm^2 sample and a resolution of 5 nm). The principal limitation of Hadamard and Fourier transform instruments is that both are sensitive to variations of the sample intensity with time.

The simplest input optics for a spectrometer employ lenses to transfer the light from the sample to the spectrometer input slit. An example of a system with refractive input optics is that by Luff and Townsend (1992). The calibration of the spectral sensitivity of a system that employs refracting input optics is not trivial where large bandwidths are involved. In general, this calibration must be done whenever any change is made in the system: either a shift in the position of the lenses or a change of slit width. This is due to the displacement of the focal point for different coloured rays at the input slit. Over the UV to near-IR (200–1000 nm) range it is not practical to produce fast lenses (i.e. $f/3$ or less) with sufficient colour correction to avoid this problem.

In addition to the problems of chromatic and geometric aberrations, a lens transfer system using practically sized lenses leaves very little space between the sample and the lens for the insertion of additional instrumentation. On the other hand, mirrors are easily produced in large diameters and do not suffer from chromatic aberration. Although mirror optics suffer from geometric aberrations, a careful choice of geometry can restrict the aberrations in such a way that light collection efficiency is unaffected. Spectrometers with completely reflective optics have been constructed by Martini *et al* (1996) and Huntley *et al* (1988). Rieser (1999) reports a design employing a combination of mirrors and lenses.

Table 1. Comparison of spectrometers. Det.: detector, PMT: photomultiplier tube, CCD: charge-coupled device, MCP: microchannel plate, PDA: photodiode array. Design described in this study is in bold typeface.

Type	Det.	$\Delta\lambda$ (nm)	Advantages	Disadvantages	References
$f/1.75$ Fourier transform	PMT	250–800	Highest throughput	Poor time resolution	Prescott *et al* (1988)
Hadamard	PMT	400–765	High throughput	Poor time resolution	Oczkowski (1992)
Interference filters + lenses	PMT	375–730 340–640	Low cost, excellent throughput	Poor IR sensitivity, low resolution, poor time resolution	Brovetto *et al* (1990), Bailiff *et al* (1977)
Absorption filters + mirror	PMT	290–600	Low cost, excellent throughput	Poor IR sensitivity, low resolution, poor time resolution	Short (2003), Jungner and Huntley (1991)
$f/7$ prism + lenses	CCD	380–880	Moderate cost	Chromatism, low resolution, poor light collection	Bakas (1984)
$f/3.8$ grating + fibre-optic	PDA	250–800	Fair UV response	Poor IR response, low light collection	Piters *et al* (1993)
$f/2$ grating + lenses	MCP(2)	200–800	High detection sensitivity	Chromatic aberration, low resolution, high cost	Luff and Townsend (1992)
$f/4$ grating + lenses	CCD	200–800	High resolution	Chromatic aberration, poor light collection	Rieser *et al* (1994)
$f/4$ grating + lens + mirror	CCD	200–800	High resolution, moderate light collection	Awkward sample placement	Rieser (1999)
$f/6$ grating + mirrors	MCP	300–750	High detection sensitivity, no chromatism	Poor IR sensitivity, poor light collection	Huntley *et al* (1988)
$f/2$ grating + mirrors	MCP	200–700	High detection sensitivity, no chromatism, good light collection	Poor IR sensitivity	Martini *et al* (1996)
$f/2$ grating + mirrors	**CCD**	**250–1000**	**Wide bandwidth, no chromatism, versatile geometry**	**Moderate detection sensitivity**	**Present study**

The design presented here uses a spherical mirror to collect the light from the sample, figure 2. A spherical mirror has the useful property that spherical aberration is absent as long as the object and image lie at the radius of curvature of the mirror. If the mirror is tilted so that the sample does not lie on the optical axis, then the reflected cone can be picked up with a small relay mirror and directed to the spectrometer slit. This off-axis configuration introduces a large amount of astigmatism into the system. However, one may adjust the position of the spectrometer input slit along the optical axis so that it is parallel to one of the astigmatic focus lines. In this way spatial resolution in the direction of the slit length is traded off for greater concentration of light along the slit width. The spot diagrams in figure 1 demonstrate this effect for a 25 cm diameter $f/1$ mirror with the source shifted along the x-axis by 2.5 cm from the centre of curvature (the optical axis is along z).

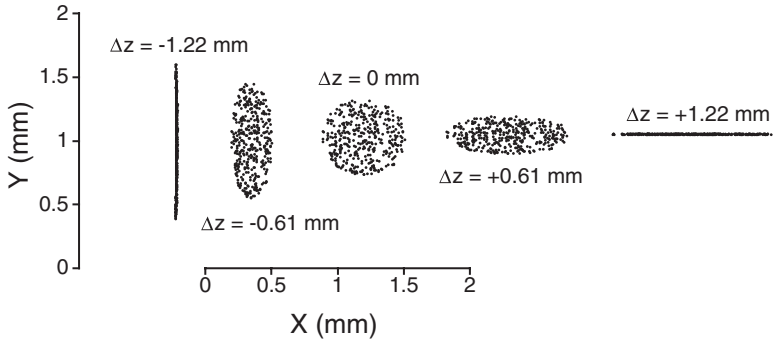

Figure 1. Ray tracing spot diagrams for a spherical 25 cm diameter $f/1$ mirror. Shown are images of a point source shifted 2.5 cm along the x-axis away from the centre of curvature at $z = 50$ cm (z is measured along the optical axis, with $z = 0$ at the mirror surface and the $\{x, y\}$-axes perpendicular to it). The image plane for the tangential focus is at $\Delta z = -1.22$ mm (far left). The sagittal focus occurs at $\Delta z = +1.22$ mm (far right).

The selected diffraction gratings were $f/2$ and $f/2.5$ concave holographic gratings with nominal bandwidths of 190–800 nm and 500–1200 nm respectively[2]. A 28 cm diameter $\sim f/1$ spherical mirror was fabricated to match the focal ratio of these gratings. The sample rests on a gimbal mounting that can be rotated through three axes and shifted vertically to achieve focus. One of the rotational axes of the gimbal mounting ensures that the sample plane is perpendicular to the optical axis, another axis aligns the planchet slot (wherein a sample is placed) so that its image is parallel to the slit. This mounting could be interchanged with a heating strip to investigate thermal effects. The étendue of the spectrometer is 0.74π mm^2 at a resolution of 25 nm, about $1/10$ the throughput of Prescott's instrument.

The flat image of the slit produced by the gratings was detected using a Hamamatsu C7041 detector head fitted with a 1044×256 pixel S7031-1008 back-thinned full-frame transfer CCD. Custom interface electronics and software were developed to acquire spectral images from the CCD.

During normal operation the CCD was operated in vertical binning mode to reduce electronic readout noise. Thermal dark count was reduced by cooling the CCD head to $\sim -40\,^{\circ}$C by affixing a dry-ice/ethanol tank. Under these conditions the dark count was approximately 8.6 electrons/pixel s^{-1}, which corresponds to $\sim$0.47 counts/pixel s^{-1}.[3]

3. Samples

Thirteen feldspar rock samples were studied. Most were obtained from Ward's supply house[4] and were cut into approximately 6 mm $\times$ 6 mm $\times$ 1 mm slices; their provenance and compositions are shown in tables 2 and 3 and figure 3. Sample K3 has been the focus of extensive studies by Short (2003). Also studied were 20 feldspar sediment separates prepared by standard methods designed to separate sand-sized K-feldspar grains (e.g. Ollerhead *et al* 2001). These samples are denoted AKHC, BIDS, CBSS, CES-5, CKDS, CTL-2, DY-23, EIDS, GP-1, IV.1, LPD, OKA-4, RHIS, SAW-95-09, SAW-97-08, SN-27, SUN, SW5-01, TAG-8 and

[2] Jobin-Yvon part numbers: 523.02.100 (190–800 nm, $f/2$), 523.01.090 (500–1200 nm, $f/2.5$). 3880 Park Avenue, Edison, NJ 08820-3097, USA.

[3] A 'count' is here defined as the smallest digital unit output from the analogue to digital converter.

[4] Ward's Natural Science Ltd, 397 Vansickle Road, St Catherines, ON, Canada.

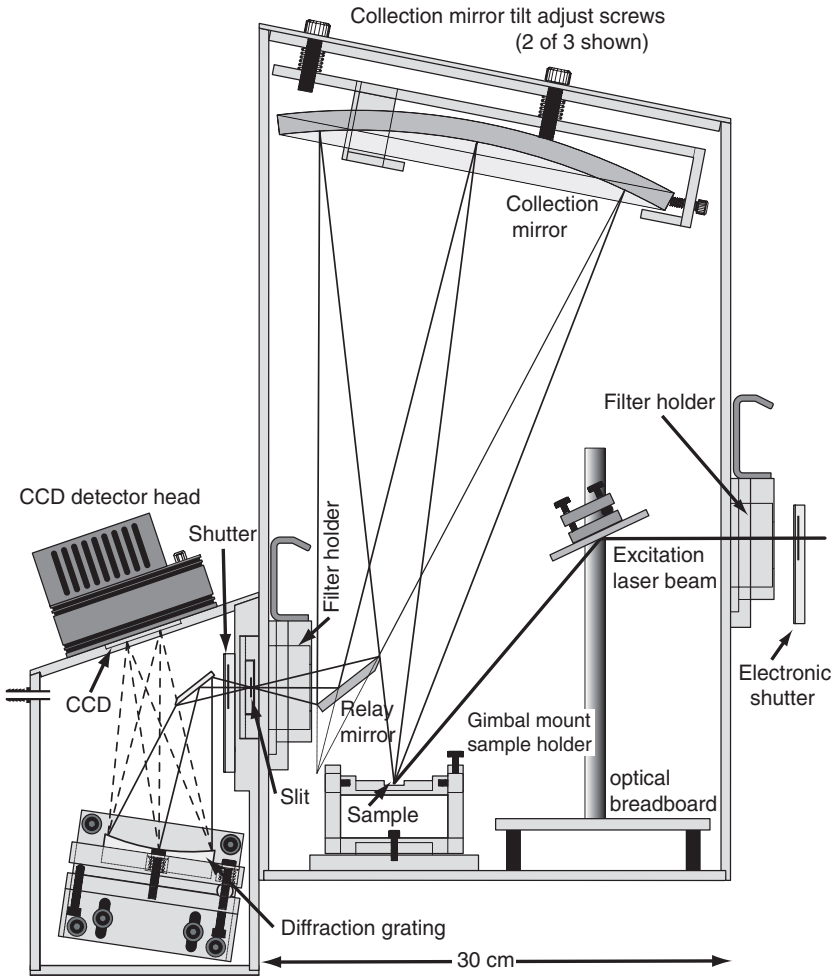

Figure 2. Layout of the spectrometer optics. The grating and detector housing have been rotated 90° about the optical axis to show the complete optical path through the instrument.

TTS; their provenances were varied and are given in Baril (2002) and Huntley and Lamothe (2001).

Major element analyses (Si, Al, K, Na and Ca) for the rock samples were performed by inductively coupled plasma emission spectroscopy (ICP-ES) whereas trace element analyses were obtained from inductively coupled plasma mass spectrometry (ICP-MS)[5].

The contents of the major, and some minor, elements are listed in table 3. Analyses were also obtained for B, Mg, Tl, Cu, Ga, Ti, Nd, Sm, Eu, Tb and Dy. The minor elements were selected on the basis that they are known to readily substitute in feldspars (Smith and Brown 1988), or they have been suggested as possible luminescence centres (Krbetschek *et al* 1997). Complete analyses are presented in Baril (2002).

The mole percentage contents of 'orthoclase', 'albite' and 'anorthite' are plotted on a ternary diagram in figure 3. It is evident from the position of K11 on this diagram that either it

[5] Analyses were performed by Acme Analytical Laboratories Ltd, 852 East Hastings Street, Vancouver, BC, V6A 1R6, Canada.

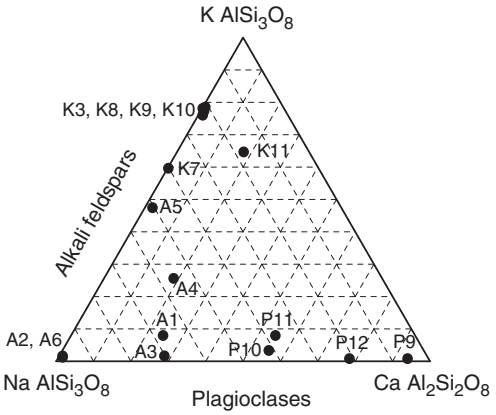

Figure 3. Ternary diagram indicating the composition of the feldspar samples. Axes represent mol% $KAlSi_3O_8$, $NaAlSi_3O_8$ and $CaAl_2Si_2O_8$.

Table 2. Cut rock sample descriptions. P9, P11 and P12 were too dim for measurement of emission spectra. These samples are included here in reference to a companion study on feldspar excitation spectra on the same samples (Baril and Huntley 2003).

Sample	Nominal composition	Appearance	Provenance
A1	Albite[b]	White with clear patches	Bancroft, ON, Canada
A2	Albite	White	Amelia Courthouse, VA, USA
A3	Oligoclase	White with black specks	Mitchell County, NC, USA
A4	Anorthoclase	Brownish black, iridescent	Larvik, Norway
A5[a]	K-feldspar	White with black specks	Bancroft, ON, Canada
A6	Albite (cleavelandite)	White	Keystone, SD, USA
K3	Orthoclase	Transparent, slightly yellow	Red Lodge, MT, USA
K7	Microcline	Light pink	Crystal peak, CO, USA
K8	Microcline (perthite)	Pink, brown and white striped exsolution bands	Perth, ON, Canada
K9	Microcline (amazonite)	Light turquoise with white stripes	Kola Peninsula, Murmansk, Russia
K10	Microcline	Translucent white with clear layers	Keystone, SD, USA
K11	Orthoclase Carlsbad twin	Orange brown, brittle	Gothic, CO, USA
P9	Anorthite in pyroxene	Grey-mottled black	Grass Valley, CA, USA
P10	Labradorite	Dark grey with blue iridescence	Nain, Labrador, Canada
P11	Andesine	Black	Essex County, NY, USA
P12	Bytownite	Greenish white, translucent	Crystal Bay, MN, USA

[a] A5 was classified as an albite by Ward's; however, the analyses and spectra strongly indicate a K-feldspar.
[b] A1 was designated 'albite' in Ward's catalogue; however, the analyses indicate that it is an oligoclase.

consists of a mixture of minerals or the Ca content is erroneously large. The Al and Si contents of K11 are close to the 9.7–10.3% and 30–32% expected for pure alkali feldspar, respectively. However, this is inconsistent with the mole percentage plagioclase implied from the Ca content relative to K and Na; one may only conclude that the Ca in this sample is associated with a Ca-rich mineral, perhaps calcite, or that the analysis is erroneous[6].

[6] The large Mn content in both these samples is consistent with the presence of calcite, for which Mn is an important impurity. However, no significant reaction was observed when sample K11 was placed in HCl as expected from calcium carbonate.

Table 3. Results of ICP-ES and ICP-MS elemental analyses (wt%) for the principal feldspar constituents and some minor elements. For complete results of analyses see Baril (2002).

Sample	Si ±0.01 (%)	Al ±0.02 (%)	K ±0.03 (%)	Na ±0.01 (%)	Ca ±0.01 (%)	Ba ±1 (ppm)	Fe ±0.01 (%)	Mn ±1 (ppm)	Pb ±0.1 (ppm)	Ce ±0.5 (ppm)	Total (%)
A1	29.14	12.24	1.02	5.55	3.29	15	0.17	26	5.0	1.0	99.2
A2	32.20	10.30	0.15	7.85	0.19	1	0.06	5	21.8	<0.5	99.5
A3	32.79	9.68	0.13	4.54	2.99	9	0.22	21	3.8	2.7	99.4
A4	28.42	9.71	3.14	4.41	2.38	62	1.98	414	1.8	208.9	98.8
A5	30.23	10.38	6.46	4.38	0.29	30	0.24	53	16.0	1.4	99.8
A6	32.20	10.15	0.18	7.67	0.19	1	0.06	35	7.6	<0.5	99.3
K3	30.94	9.56	9.38	1.79	0.16	75	0.05	4	5.5	4.6	99.3
K7	32.50	8.94	6.93	2.97	0.01	11	0.21	10	9.8	1.7	99.1
K8	31.11	9.67	9.50	1.76	0.10	14	0.17	13	11.9	<0.5	99.1
K9	31.14	9.64	9.88	1.77	0.01	48	0.03	4	57.6	<0.5	99.3
K10	31.18	9.60	10.06	1.73	0.05	3	0.03	5	7.9	0.9	99.4
K11	28.64	9.30	8.08	1.45	2.27	141	0.58	397	11.6	26.9	95.2
P9	20.30	10.96	0.03	0.39	8.48	31	6.15	1071	0.5	1.7	99.3
P10	26.25	13.98	0.37	3.47	7.33	45	0.30	23	0.9	12.6	99.3
P11	24.78	12.53	1.00	3.18	7.44	28	1.68	83	1.5	36.2	98.5
P12	23.27	15.65	0.07	1.84	10.48	45	0.36	47	0.5	1.4	98.8

4. Emission spectra using 1.43 eV (IR) excitation

The excitation source consisted of a Ti–sapphire laser tuned to 1.43 eV (865 nm), with a beam power in the range of ∼10–50 mW cm^{-2} at the sample. Filters were used on the spectrometer input to absorb scattered excitation photons and to prevent overlap of the first- and second-order spectra. Three passbands were defined: the 'red' band (750–600 nm), the 'visible' band (600–350 nm) and the 'UV' band (350–275 nm). The filter combinations used to define these bands were: 'red': two CVI[7] 500–750 nm bandpass filters, 875 and 830 nm Raman notch filters[8]; 'visible': one 2.2 mm thick Schott BG-39 filter; and 'UV': one 3 mm thick Schott UG-11 filter. The excitation was selected at 865 nm to make effective use of the 875 nm notch filter while remaining close to the excitation resonance of feldspars at 1.44 eV. The spectra for each defined passband were measured separately on the same sample aliquot, integrating for 10–20 s of illumination. Before each measurement a sample was bleached under a sun lamp and then given a 750 Gy Co^{60} γ-dose at ∼10 Gy h^{-1}. The spectra were corrected for CCD thermal dark count and normalized for the spectrometer response (filters included). The 'UV' and 'red' band data were then scaled to match the 'visible' passband data where they overlapped. The intensities were then scaled for display on an energy scale.

The measurements immediately following irradiation were performed within 5 h of removal from the γ-source. Spectral measurements were repeated on the same aliquots after they had been re-irradiated and then heated at 120 °C for 16–20 h.

Generally, a 0.6 mm or smaller slit was used whenever possible, providing an effective bandwidth of 15 nm at 500 nm. A background level was determined for each aliquot and subtracted; the background was determined by a measurement made after an additional 60 s of illumination. The data were smoothed by resampling, averaging over groups of five CCD columns[9].

[7] CVI Laser Corporation, 200 Dorado Place SE, Albuquerque, NM 87123, USA. Filter: SPF-800-1.00.

[8] Physical Optics Corporation, 20600 Gramercy Place, Building 100, Torrance, CA 90501-1821, USA. Filters no 848 ($\lambda = 875$ nm) and no 703 ($\lambda = 830$ nm).

[9] A bandwidth of 25 nm corresponded to roughly ∼10 CCD columns at 500 nm.

In figure 4 the spectra for the unpreheated samples are drawn in bold black and the spectra for the preheated samples are drawn in bold grey. The spectra for EIDS, IV.1, LPD, RHIS and SAW-95-09 were selected as being representative of the spectra observed for the feldspar separate samples (spectra for the other feldspar separates may be found in Baril (2002)).

4.1. Principal features of the spectra

The data support the conclusions of earlier work that, in preheated samples, the 2.2 eV band is dominant in plagioclases and the 3.1 eV band dominates in alkali feldspars. The 1.7 eV emission band is well known from TL emission spectra (Huntley *et al* 1988, Prescott and Fox 1993, Visocekas and Zink 1999) where it predominates in low-potassium feldspars. This emission band has been attributed to Fe^{3+}, which substitutes for Al^{3+} in tetrahedral sites, on the basis of excitation spectra (Telfer and Walker 1978).

The position of the 1.7 eV emission band varies from sample to sample and disappears upon heating the sample at 120 °C for 16 h. The exception is microcline K7, for which the 1.7 eV emission does not completely vanish after the preheat. In plagioclases the peak position has been observed to vary between 1.8 and 1.6 eV (Geake *et al* 1977). Mora and Ramseyer (1992) found a correlation between the peak position of the 1.7 eV cathodoluminescence and the Ca content in plagioclases; positions ranged from 1.80 eV for anorthite to 1.67 eV for andesine. Dütsch and Krbetschek (1997) showed a nice correlation between the peak position in radiophosphorescence and the potassium content. Alternative suggestions have been made that the position is determined by the relative amounts of Fe^{3+} in T_1 and T_2 sites following fluorescence measurements (Slaats *et al* 1991) and cathodoluminescence measurements (Finch and Klein 1999), though these suggestions appear to conflict. Krbetschek *et al* (2002) showed in a comprehensive study that the peak energy depends on feldspar composition as well as the excitation mechanism; they suggested that the site occupancy of the Fe^{3+} and varying Fe–O bond distances were responsible.

A shift of the violet (3.1 eV) emission band towards UV by up to 0.11 eV following the preheat was observed for many samples. This shift was almost ubiquitous in the feldspar separates but was not observed clearly in the cut rock samples.

Upon preheating, the intensities of the yellow–green and UV bands usually decreased by a relatively larger amount than that of the violet emission. However, a sufficient number of samples departed from this behaviour that it cannot be established as a rule. In particular the UV peak(s) were observed to increase relative to the violet in K3, CBSS and RHIS, whereas the yellow–green emission increased relative to the violet in A6, RHIS and SN-27.

4.2. Correlation of the spectral features with sample compositions

A plot of the ratio of the [violet] intensity to the [yellow–green + violet] intensity versus the ratio of the [K] content to the [K] + [Na] content, [K]/([K] + [Na]), indicates a correlation between K-rich samples and samples for which the violet predominates over yellow–green luminescence (figure 5, left). Sample K8 exhibits the greatest departure from this rule; the analysis clearly shows it to be a K-feldspar yet the yellow–green emission predominates in this sample.

The intrinsic intensity was dimmest in the Ca-bearing samples, particularly the plagioclases (figure 5, right). The intrinsic intensity is here defined as the intensity of the brightest emission band in the sample relative to the ratio of the intensity of the violet emission band of sample K3. This quantity is useful because the variation in intensity between different samples is often much larger than the variation in the relative intensity of emission bands

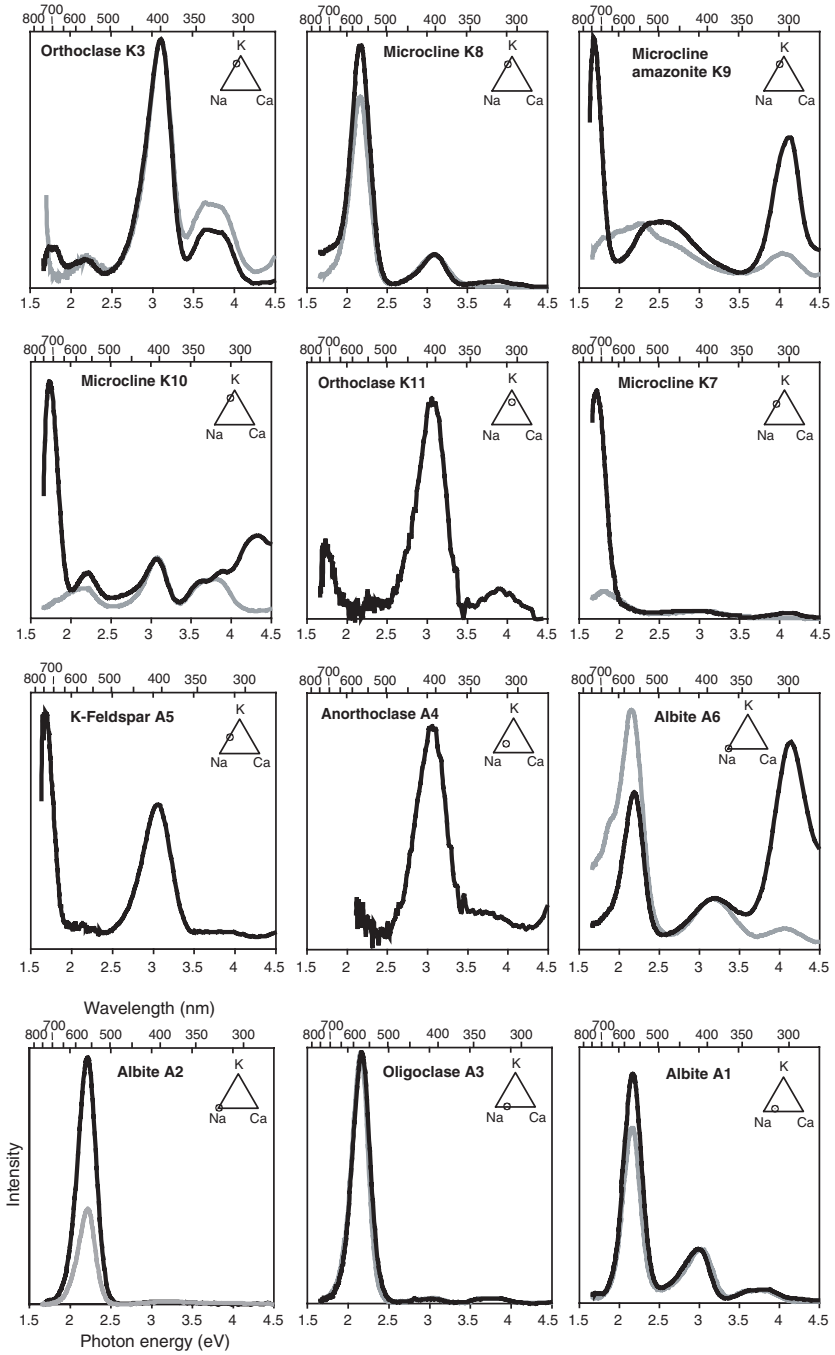

Figure 4. Emission spectra for the feldspars under 1.4 eV excitation. Preheated sample data in grey, unpreheated sample data in black. Data are scaled to the same intensity for the 3.1 eV band. The inset ternary diagrams show the major element compositions. Emission spectra for EIDS, IV.1, LPD, SAW-95-09 and RHIS are representative of the spectra obtained for the other feldspar separate samples.

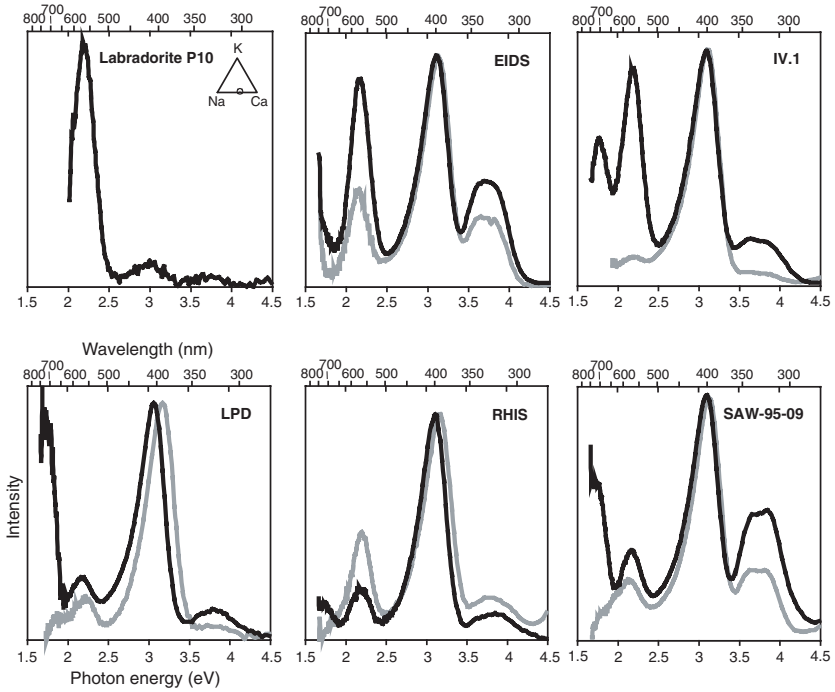

Figure 4. (Continued.)

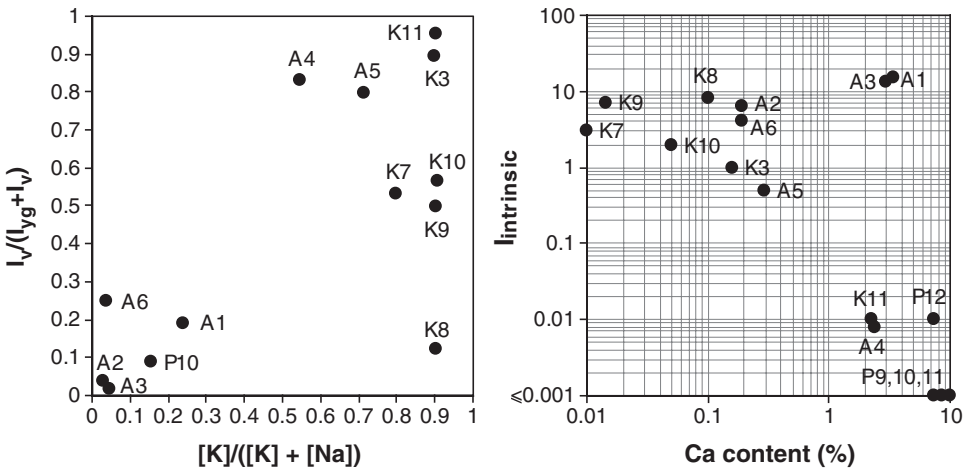

Figure 5. Left: correlation of the intensity of the violet emission band (I_v) relative to the intensity of the yellow–green band (I_{yg}) with the K molar content [K] relative to the Na molar content [Na]. Right: correlation of the intrinsic intensity, $I_{intrinsic}$ (see text for definition), with the Ca content (% wt).

in a single sample. For example, if one plots the absolute intensity of the violet or yellow–green emission versus Ca content, the same general trend towards lower intensity at higher Ca content is observed for both emission bands. This is in agreement with the observations made by Spooner (1992).

Correlations were sought between the individual absolute emission band intensities and intrinsic intensities with the abundances of all the measured impurity elements. Few correlations were found, and trends were noticed only for Mn, Fe, Pb and some weaker correlations with the lanthanide element contents. Graphs of the correlations for some of these elements can be found in Baril (2002).

Tarashchan (1978) observed a band near 4.4 eV in an oligoclase and two microclines that was attributed to Pb^{2+}. The amazonite microcline K9 had the largest Pb content and also the brightest emission at 4.1 eV. High Pb contents are not unusual in amazonites which derive their bright green colour from Pb^{2+} centres (Smith and Brown 1988). The 4.1 eV band was only clearly observed in two other samples, A6 and K10, both of which did not exhibit unusually high Pb contents. Although no clear correlation was observed between Pb content and the 4.1 eV band, the Pb content appeared to be positively correlated with the intrinsic intensity.

A weak anti-correlation was noted between the contents of the lanthanides (Sm, Tb, Nd, Ce) and the intrinsic intensity of the samples. It is impossible to say which of these elements is responsible for this effect because the abundances of these elements are strongly correlated.

Mora and Ramseyer (1992) and Telfer and Walker (1978), using cathodoluminescence, have found a correlation between Mn content and the intensity of the yellow–green emission. This correlation was not observed in the present samples for IR stimulated luminescence. In fact, there appears to be an anti-correlation between Mn and Fe contents and the intensities of all emission bands. It is impossible to tell whether this is due to the presence of Mn, Fe or both, because there is a very strong positive correlation between the Mn and Fe contents.

5. Variation of the emission spectrum during shinedown

In the brightest of the samples it was possible to measure the emission spectrum several times during a short excitation by 1.43 eV photons. In this way, the rates of decay of the violet and yellow–green emission bands as a function of excitation time could be compared.

Each spectrum was integrated for 4 s using a beam power of $\sim$100–300 mW cm^{-2}, for a total of 80 s (20 time slices). A spectrometer bandpass of 25 nm was used. The spectra for one sample and decay curves for the two emission bands for several samples are shown in figure 6.

The peak positions did not shift during the decay. The rates of decay of the yellow–green emission were similar to those for the violet emission, but not identical. For several samples, the decay curve approaches $1/t$, although Becquerel's decay law, $I(t) = I_0/(1 + t/t_0)^{\alpha}$, is more generally observed. Such a fit has been reported by Bailiff and Poolton (1991) for a sanidine immediately following laboratory irradiation, and by Bailiff and Barnett (1994) for an orthoclase at 160 and 290 K. Much more information can be found in Baril (2002).

6. Effect of the excitation photon energy on the emission spectrum

With the simplest model, in which electrons are excited to the conduction band, one expects that the luminescence spectrum should not be affected by the energies of the excitation photons, which should only affect the rate at which traps are emptied. The shape of the spectrum should remain unchanged as long as the relative concentration of available recombination centres is fixed. Since the shape of the luminescence excitation spectrum is not strongly dependent on whether the 3.1 or 2.2 eV emission bands are measured (Baril and Huntley 2003), a correlation between the trap(s) associated with the 1.44 eV resonance and these emission bands is not expected. The emission spectrum may depend on the excitation photon energy if the sample consists of segregated mineral domains exhibiting different luminescence

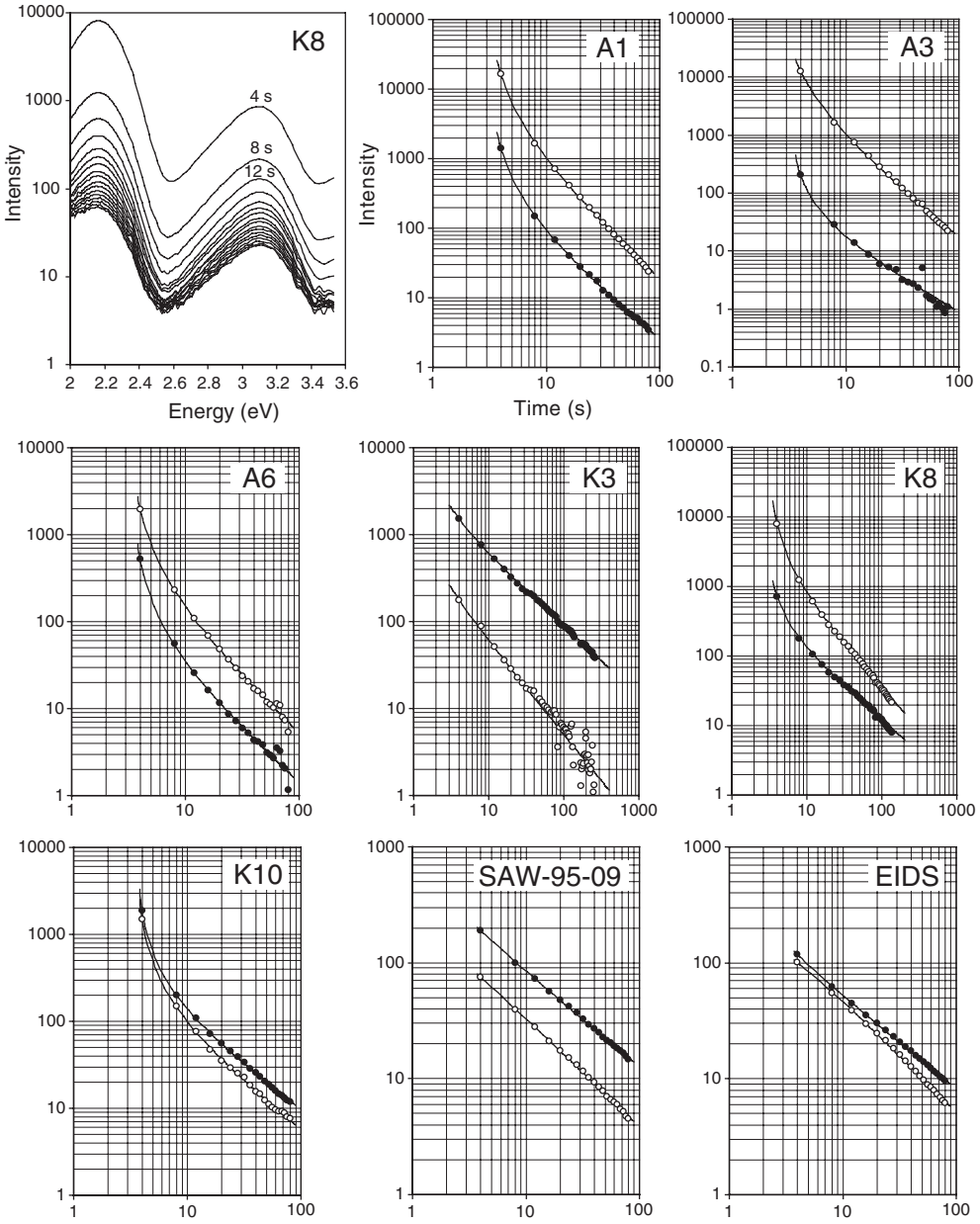

Figure 6. Top left: emission spectra as a function of 1.4 eV illumination time (t) for K8. The dose was 1100 Gy and there was no preheat. Remaining: violet emission (solid circles) and yellow–green emission (open circles) peak intensity as a function of illumination time. Lines through the data are fits to $I_0/(1 + t/t_0)^{\alpha}$, with I_0, t_0 and α parameters in the fits.

characteristics. Since this is often the case in natural feldspars, especially in alkali feldspars, an investigation of the effect of varying excitation energy on the emission spectrum was warranted.

The use of a single aliquot for all the measurements at different excitation energies was essential because the luminescence spectrum can vary greatly from aliquot to aliquot when using cut rock samples. K3, for example, was particularly problematic in this respect, with

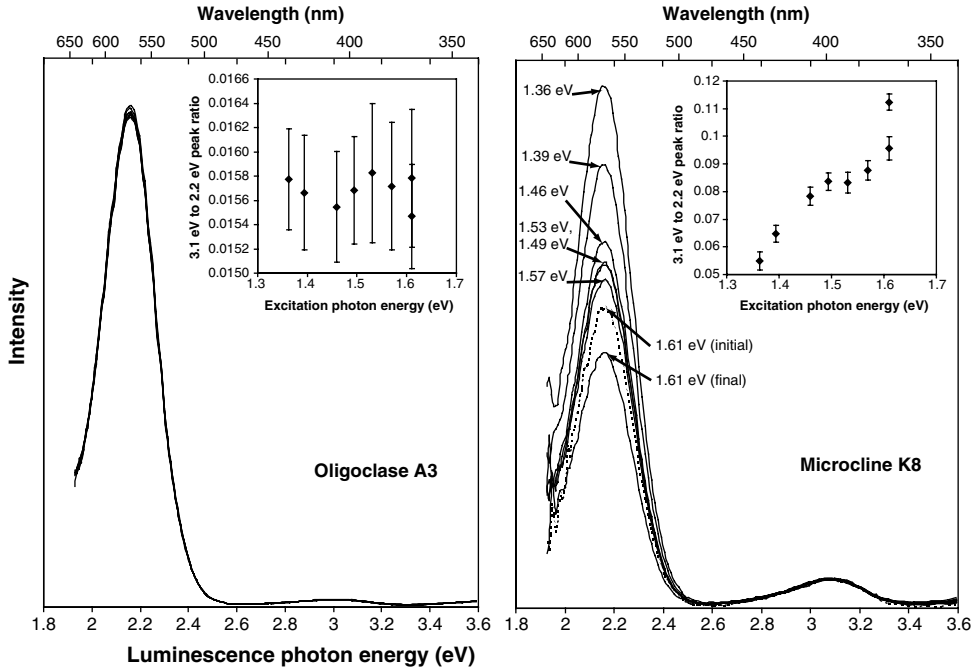

Figure 7. Effect of varying the excitation photon energy on the visible emission spectrum for A3 and K8. Spectra normalized to the 3.1 eV intensity; note that in A3 the emission spectra at all excitation energies scale almost perfectly. Insets: ratio of the violet to the yellow–green peak intensity as a function of excitation photon energy.

the 570 nm emission being prominent in some aliquots and almost absent in others. The requirement that little decay in the luminescence occur over the measurement was necessary to avoid the effect of the differing draining rates of the different luminescence bands. These restrictions meant that only the violet (3.1 eV) and yellow–green (2.2 eV) bands could be easily compared. Only three samples had sufficiently bright 3.1 and 2.2 eV bands to allow an accurate comparison to be made: albite A1, oligoclase A3 and microcline K8. The spectra were measured for excitation energies between 1.36 and 1.61 eV using a tunable Ti–sapphire laser with a power of 3–6 mW on the sample. The measurement of all the excitation spectra produced a cumulative decay in the luminescence of less than 2% in A1 and A3 and 18% in K8.

The emission spectra as a function of excitation energy are shown in figure 7 for samples A3 and K8. The excitation photon energy clearly has no effect on the spectrum of A3 in the range 1.9–3.6 eV. Sample K8 shows the greatest departure from the ideal behaviour, with the yellow–green emission being relatively greater than the violet at smaller excitation energies. A similar, much smaller trend was also noted in the data for A1. Although the luminescence decay over the measurement period affected the ratio of the violet to yellow–green emission in K8, the effect of the decay was in the opposite direction to that due to the excitation energy (the higher excitation energy spectra were measured first). For this reason, the effect of the excitation energy is probably underestimated.

The most satisfactory explanation for the large effect of the excitation energy on the emission spectrum of K8, and little if any effect on A1 and A3, is found in the morphology of K8, which is a classic perthitic microcline containing exsolved phases of orthoclase and albite. The association of the violet and yellow–green emissions to regions of K-feldspar and

Na-feldspar respectively has been demonstrated for this sample by Baril (2003). In A3 and A1 on the other hand, the violet and yellow–green emission as well as the potassium and sodium content were found to be evenly distributed in those regions where any emission is present. The difference in the excitation response of the violet and yellow–green bands in K8 is most easily interpreted as arising from a mixture of K- and Na-feldspar in the sample. This is also consistent with the excitation spectra measured for K8; this sample produced the greatest difference between the excitation spectra measured for the violet and yellow–green emission bands separately (Baril and Huntley 2003). Not surprisingly, A1 demonstrated very little variation in the excitation response spectra for the violet and yellow–green emission bands.

7. Post-irradiation phosphorescence

The phosphorescence spectra are quite different; these are shown in figure 8 for five feldspars. Measurements on three feldspar sediment separates (AKHC, GP-1 and SAW-95-09) produced similar phosphorescence spectra. The samples were given a γ-dose of 2770 Gy over 11 days and measured within 2 h of removal from the γ-source (no preheat). For the data between 690–1000 nm the 500–1200 nm grating was used with an effective bandpass of 25 nm; the shorter wavelength data were obtained using the 200–800 nm grating and a bandpass of 15 nm or less. An integration time of 20 s was used at each temperature. For the long-wavelength data, no filters were used to separate out the first and second diffraction orders; instead the inferred second-order spectrum was subtracted from the data. In the case of A6 and K9 a long-pass filter was used to absorb the strong UV emission when measuring the long wavelengths.

Several features stand out in these spectra. The 3.1 and 2.2 eV bands that dominate the 1.43 eV excited luminescence are absent or strongly subdued in the phosphorescence spectra. Instead the emission is dominated by bands near 1.38, 1.65 eV, a broad band centred at 2.7 eV (the spectra of K8 and A6 are exceptions) and in two cases (A6 and K9) UV bands at 4.2 and 4.5 eV. The intensities of the 1.38 eV, 2.7 eV and UV bands increase with temperature at nearly the same rate, but much faster than that of the 1.65 eV band.

A phosphorescence/TL emission band near 1.38 eV has been reported by Rieser (1999) and is hinted at in the TL spectra of Krbetschek and Rieser (1995). A bright band near 1.44 eV has been seen in the radioluminescence of K-feldspar (Trautmann *et al* 1999), but there is no trace of it in the present data.

The 2.7 eV band is likely to be the same band observed in the TL of feldspars near 2.7 eV by Huntley *et al* (1988) and Prescott and Fox (1993). Krbetschek and Rieser (1995) found two well-resolved phosphorescence bands near 2.5 eV as well as a band near 2.75 eV. The 2.7 eV phosphorescence band is subdued or absent in microcline K8 and albite A6. Instead, other bands are found between 2.1 and 3 eV. In the feldspar separate samples, AKHC, GP-1, SN-27, EIDS and IV.1, this band appeared between 2.5 and 2.6 eV. Spectra for sample AKHC are shown in figure 9.

The red/IR, 1.65 eV phosphorescence band is likely to be the same as the 1.7 eV band observed in the 1.43 eV excited luminescence. The width of these emission bands is $\sim$0.18 eV in both cases. Krbetschek *et al* (2002) found that the peak energy of the red/IR band differed in cathodoluminescence, radioluminescence and photoluminescence. In view of this, the peak shift of the red/IR band observed between IR stimulated luminescence and phosphorescence is not entirely surprising.

The 4.2 and 4.5 eV phosphorescence is strongest in the samples in which the 4.1 eV band is present in IR stimulated luminescence, so that these bands are probably due to the same recombination centre(s).

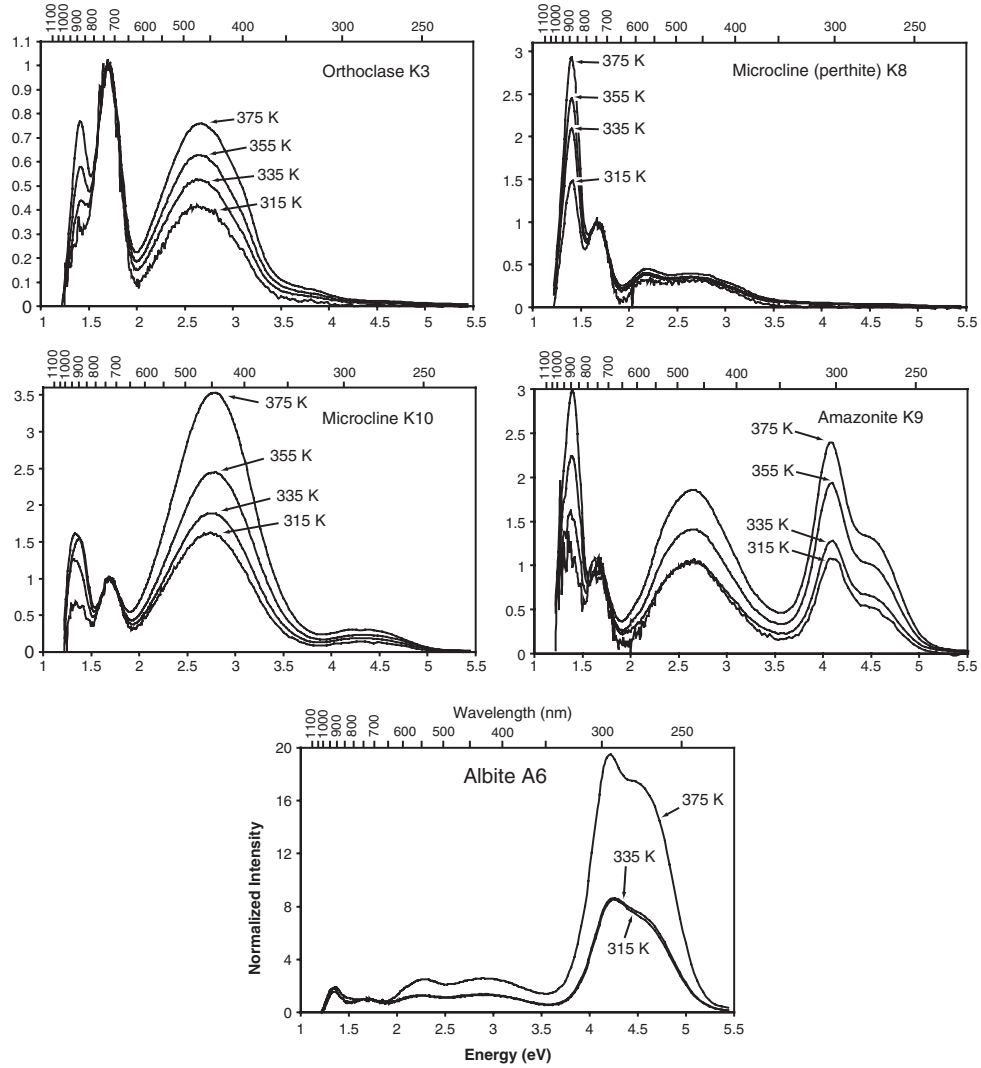

Figure 8. Temperature dependence of the prompt phosphorescence spectra. Spectra have been scaled to the intensity of the 1.65 eV emission peak (25 nm resolution).

8. Time dependence of the phosphorescence

Figure 9 shows how the phosphorescence intensity decreases with time for the three main emission bands. Three representative samples are shown; other samples exhibited similar time dependence. Prior to measurement, the samples were given a 2770 Gy γ-dose over 11 days. The sample temperature was held at 120 °C during a measurement.

The decay of the luminescence follows Becquerel's law with the power-law exponent close to unity in all cases; fitting parameters are given in table 4. The exponent for the 1.38 eV band is consistently lower, 0.95–1.05, than those for the 2.53 and 1.65 eV bands, both of which are close to 1.10–1.15 (this is readily seen in the decay curves of figure 9). It is interesting to note that the relative intensities of the three bands are nearly constant during this decay with time, but varied considerably as the temperature was increased.

Table 4. Decay exponent α in the fit of the phosphorescence decay to Becquerel's equation, $I_0/(1+t/t_0)^{\alpha}$.

Sample	Emission (eV)	α
AKHC	1.38	0.990 ± 0.006
	1.65	1.148 ± 0.006
	2.53	1.148 ± 0.005
SAW-95-09	1.38	0.948 ± 0.004
	1.65	1.128 ± 0.006
	2.53	1.083 ± 0.005
GP-1	1.38	1.045 ± 0.005
	1.65	1.148 ± 0.005
	2.53	1.137 ± 0.004

9. Post-illumination phosphorescence

The phosphorescence spectrum of a sample following 1.4 eV excitation was different from the phosphorescence following irradiation. Although the distribution of trapped charges in the lattice is likely to be different for the two cases, one might expect that the emission bands would be similar in both situations. Although no new emission bands were found, the relative intensities of the bands were quite different from those found in the post-irradiation phosphorescence.

Spectra were obtained for five feldspar samples: albite A6, perthite K8, orthoclase K3 and microclines K9 and K10. The 500–1200 nm grating was used with a 25 nm bandpass. The samples were given a 1450 Gy γ-dose over 139 h and measured within 4 h of the end of irradiation. The samples were excited with 1.43 eV light for 1 s, and then (once the illumination shutter closed) the phosphorescence was measured for 3 s during which it decayed to an unmeasurable level. The measurement was repeated 20 times so that the change of the phosphorescence as the traps were emptied could be noted. The phosphorescence due to the γ-dose was negligible. The spectra and decay curves for the principal emission bands are shown in figure 10.

The dominant emission band is in the IR, centred between 1.265 and 1.38 eV (900–980 nm). Emission bands at 1.7 and 2.1 eV are also present but the broad 2.7 eV emission band that predominated in the post-irradiation phosphorescence is completely absent. The relative rate of decrease of the emission band intensities varies greatly between samples so that no generalization can be made in this regard.

10. Discussion and conclusions

Table 5 lists the main emission bands observed and an indication of the frequency of their occurrence with different excitation mechanisms. It is evident from comparisons of the various spectra that the notion of the recombination centres being largely independent of the electron traps cannot be correct. If this were true, we would expect the spectra for each excitation mechanism to be generally similar; that is, any electron in the 'conduction band' would have access to all recombination centres. However, it appears that even when the excitation mechanisms are similar, as in the post-illumination and post-irradiation phosphorescence, the emission spectra differ considerably. These results rule out models involving excitation from the excited level of the trap to the conduction band, such as the 'thermally assisted transfer' model due to Hütt *et al* (1988) to explain the IR stimulated luminescence. One possible

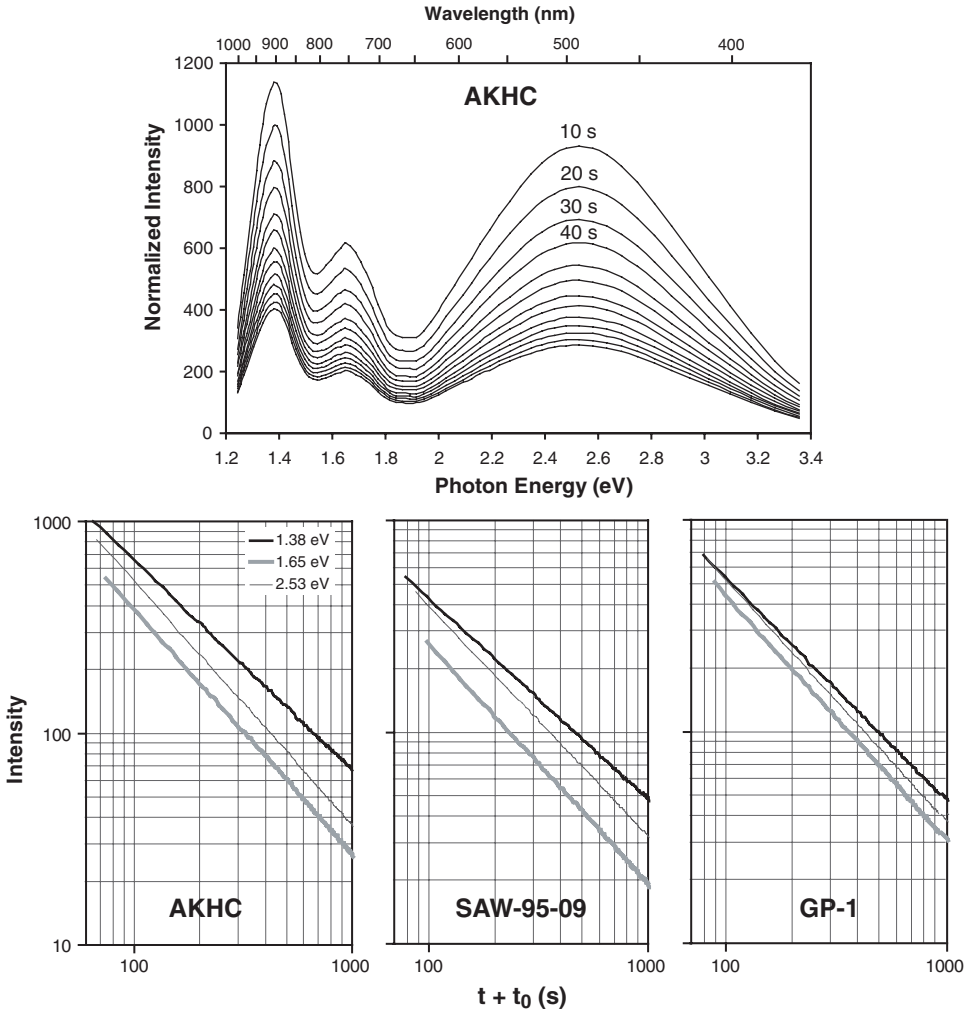

Figure 9. Top: phosphorescence emission spectrum as a function of time for sample AKHC at 120 °C; each curve represents a 10 s increment. Bottom: phosphorescence decay with time for the three emission bands. Decay curves have been shifted on the time axis by the fitting parameter t_0 to display adherence to Becquerel's law, $I(t) = I_0/(1+t/t_0)^{\alpha}$. Intensities have been corrected for the second-order spectrum and corrected for system response.

alternative model is hopping of the electron between closely spaced defects, or 'localized defect complexes', as has been suggested by Karali *et al* (2000) in zircons. Another possibility is direct tunnelling of the electron from the excited level of the trap to the luminescence centre.

A case can be made that the ∼2.7 eV band results from the recombination of an electron in the conduction band or a hole in the valence band. The 2.7 eV band is seen after high-energy excitation, but not after 1.4 eV excitation. Given the suggested interpretation, this is consistent with our previous conclusion that the electron is not excited into the conduction band during optical excitation out of the excited state of the principal trap. It is also worth noting that at 1 eV, the width of the 2.7 eV band is much greater than any other emission band measured in feldspars. Huntley *et al* (1988) noted that in TL, the 2.7 eV band is usually weak, but in

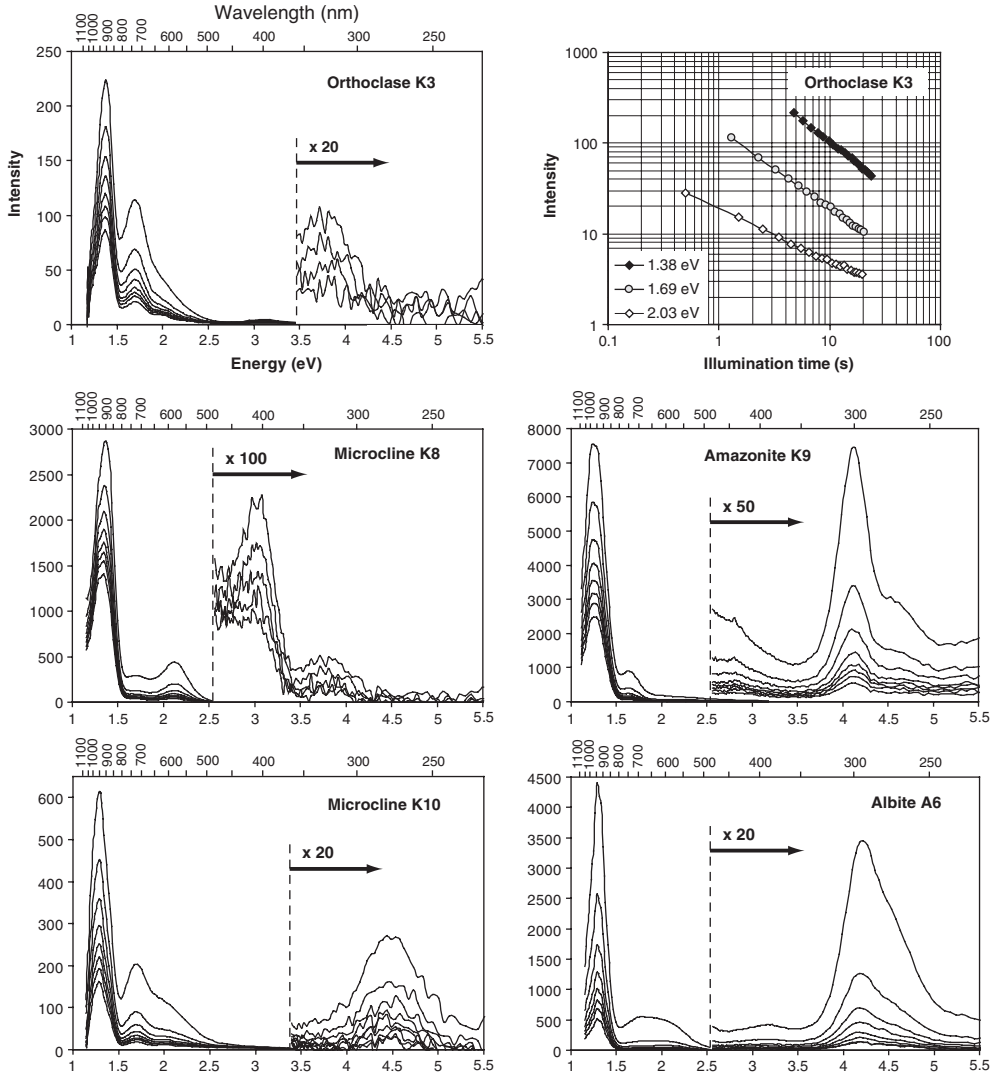

Figure 10. Post-illumination phosphorescence at 1.4 eV as a function of illumination time. Each curve (in black) represents the phosphorescence after 1 s of 1.4 eV illumination. The decay curves for the three brightest emission peaks in K3 are shown; the curves have been shifted in time to show adherence with Becquerel's decay law. The form of the decay is similar in other samples, although the relative rates of decay for the emission bands vary greatly.

their oligoclase P1 the 2.7 eV band constituted the dominant emission, making this sample the intrinsically brightest measured. Under optical excitation, however, P1 was a relatively dim sample (Huntley *et al* 1989).

The 1.27–1.38 eV phosphorescence emission has been scantily reported (Rieser 1999) and requires further investigation. It is tempting to associate this band with recombination in the principal trap, with the shift to lower energy explained by a Stoke's shift. However, this interpretation conflicts with the work of Trautmann *et al* (1999) who attribute the 1.44 eV radioluminescence (RL) emission to recombination in the principal trap. The phosphorescence

Table 5. The main emission bands observed, indications of occurrence with different excitations, and attributions where determined. The IR and red/IR bands may be composed of two or more peaks. Key: 0 = not observed, w = observed but very weak, ∗ = uncommon, ∗∗ = common, ∗ ∗ ∗ = ubiquitous, n.o. = not observable, ? = not measured. Thermoluminescence (TL) observations of Huntley *et al* (1988), Prescott and Fox (1993) and Rendell *et al* (1995). Radioluminescence (RL) observations of Trautmann *et al* (1999, 2000), Erfurt and Krbetschek (2003) and Rendell and Clarke (1997).

Emission	Peak energy (eV)	Peak λ (nm)	TL	RL	1.4 eV exc.	Phosphorescence after γ-irr.	Phosphorescence after 1.4 eV exc.	Attribution
IR	1.27–1.38	900–980	?	*	n.o.	***	***	
IR	1.46	855–885	?	***	n.o.	0	0	
Red/IR	1.65–1.82	730	**	***	**	***	***	Fe^{3+} in T site
Yel./gr.	2.2	570	***	*	***	*	**	Mn^{2+} in M site
Green	2.5–2.7	460–500	*	*	0	***	0	
Violet	3.0–3.1	400–420	***	***	***	*[a]	***w	
UV	3.65	340	0	0	**	0	0	
UV	3.85	320	**	0	**	*	*w	
UV	4.1	300	0	0	*	*	*w	Perhaps Pb^{2+}
UV	4.3	290	**	***	*	*	**w	
UV	4.5	275	**	0	?	*	0	

[a] Rieser (1999).

generally arises from electrons in shallow traps being thermally excited to the conduction band, so one expects the energies of the emission bands to be the same for both phosphorescence and radioluminescence.

There appears to be a clear correlation between the ratio of the intensities of the violet and yellow–green IR stimulated luminescence emission bands and the [K] to [Na] ratio. This is analogous to what had been seen by Prescott and Fox (1993) using TL. Correlations of minor elemental contents with the luminescence emission bands were largely inconclusive.

Future work on correlating elemental contents and luminescence behaviour should place more attention on the problem of obtaining absolute sample intensities. It should be emphasized that the intrinsic intensities given in this study are only approximate due to several factors. The slight sensitivity difference between different measurements due to changes in the spectrometer setup is probably the least significant problem and likely contributes less than a factor of two to the spread in intrinsic intensities. Likewise, the size of the sample is not a significant factor because the spectrometer slit was overfilled by the luminescence from the sample in all cases. The large variation in the transparency between samples is the most significant issue. Some plagioclase samples were almost opaque whereas other samples, such as K3, were almost transparent. This problem may be minimized in future work by thinning the samples to a uniform thickness. Once thinned, the transmissivity of the samples could be measured and corrections applied for the absorption of the excitation and emission.

Acknowledgments

The following are thanked for providing samples or help with collecting them: M Auclair, W Blake, J J Clague, S R Dallimore, R J Fulton, L Groat, S R Hicock, H Jungner, M Lamothe, O B Lian, Y A Mochanov, J Ollerhead, P A Shane, M A Short, P Soloveyeev, S van Heteren and S A Wolfe. We wish to express our gratitude to J R Prescott for his comments on the

manuscript. This research was supported by the Natural Sciences and Engineering Research Council of Canada.

References

Aitken M J 1998 *An Introduction to Optical Dating* (Oxford: Oxford University Press)
Bailiff I K and Barnett S M 1994 *Radiat. Meas.* **23** 541–5
Bailiff I K, Morris D A and Aitken M J 1977 *J. Phys. E: Sci. Instrum.* **10** 1156–60
Bailiff I K and Poolton N R J 1991 *Nucl. Tracks Radiat. Meas.* **18** 111–8
Bakas G V 1984 *Radiat. Prot. Dosim.* **9** 301–5
Baril M R 2002 Spectral investigations of luminescence in feldspars *PhD Thesis* Simon Fraser University, Burnaby, BC, Canada
Baril M R 2003 CCD imaging of the infra-red stimulated luminescence of feldspars *Radiat. Meas.* at press
Baril M R and Huntley D J 2003 Optical excitation spectra of trapped electrons in irradiated feldspars *J. Phys.: Condens. Matter* **15** 8011
Brovetto P, Delunas A, Maxia V, Spano G and Cortese C 1990 *Nuovo Cimento* **12** 331–7
Dütsch C and Krbetschek M R 1997 *Radiat. Meas.* **27** 377–81
Erfurt G and Krbetschek M R 2003 *Radiat. Meas.* **37** 505–10
Finch A A and Klein J 1999 *Contrib. Mineral. Petrol.* **135** 234–43
Geake J E, Walker G and Telfer D J 1977 *Phil. Trans. R. Soc.* A **285** 403–8
Huntley D J, Godfrey-Smith D I and Haskell E H 1991 *Nucl. Tracks Radiat. Meas.* **18** 127–31
Huntley D J, Godfrey-Smith D I, Thewalt M L W and Berger G W 1988 *J. Lumin.* **39** 123–36
Huntley D J and Lamothe M 2001 *Can. J. Earth Sci.* **38** 1093–106
Huntley D J, McMullan W G, Godfrey-Smith D I and Thewalt M L W 1989 *J. Lumin.* **44** 41–6
Hütt G, Jaek I and Tchonka J 1988 *Quat. Sci. Rev.* **7** 381–5
Jungner H and Huntley D J 1991 *Nucl. Tracks Radiat. Meas.* **18** 125–6
Karali T, Can N, Townsend P D, Rowlands A P and Hanchar J M 2000 *Am. Mineral.* **85** 668–81
Krbetschek M R, Götze J, Dietrich A and Trautmann T 1997 *Radiat. Meas.* **27** 695–748
Krbetschek M R, Götze J, Irmer G, Rieser U and Trautmann T 2002 *Mineral. Petrol.* **76** 167–77
Krbetschek M R and Rieser U 1995 *Radiat. Meas.* **24** 473–7
Luff B J and Townsend P D 1992 *Meas. Sci. Technol.* **3** 65–71
Martini M, Paravisi S and Liguori C 1996 *Radiat. Prot. Dosim.* **66** 447–50
Mora C I and Ramseyer K 1992 *Am. Mineral.* **77** 1258–65
Oczkowski H L 1992 *Acta Phys. Pol.* A **82** 367–75
Ollerhead J, Huntley D J, Nelson A R and Kelsey H M 2001 *Quat. Sci. Rev.* **20** 1915–26
Piters T M, Meulemans W H and Bos A J J 1993 *Rev. Sci. Instrum.* **64** 109–17
Prescott J R and Fox P J 1993 *J. Phys. D: Appl. Phys.* **26** 2245–54
Prescott J R, Fox P J, Akber R A and Jensen H E 1988 *Appl. Opt.* **27** 3496–502
Rendell H M and Clarke M L 1997 *Radiat. Meas.* **27** 263–72
Rendell H M, Townsend P D and Wood R A 1995 *Phys. Status Solidi* b **190** 321–30
Rieser U 1999 Spektrometrie an Feldspäten als Beitrag zur aufklärung physikalischer Grundlagen der Lumineszenz-datierungstechnik *PhD Thesis* Ruprecht-Karls-Universität, Heidelberg (in German)
Rieser U, Krbetschek M R and Stolz W 1994 *Radiat. Meas.* **23** 523–8
Short M A 2003 An investigation into the physics of the infrared excited luminescence of irradiated feldspars *PhD Thesis* Simon Fraser University, Burnaby, BC, Canada
Slaats P G G, Dirksen G J and Blasse G 1991 *Mater. Chem. Phys.* **30** 19–23
Smith J V and Brown W L 1988 *Feldspar Minerals* 2nd edn, vol 1 (New York: Springer)
Spooner N A 1992 *Quat. Sci. Rev.* **11** 139–45
Tarashchan A N 1978 *Luminescence of Minerals* (Kiev: Naukova Dumka) referred to in Marfunin A S 1979 *Spectroscopy, Luminescence and Radiation Centres in Minerals* (New York: Springer) p 237
Telfer D J and Walker G 1978 *Mod. Geol.* **6** 199–210
Trautmann T, Krbetschek M R, Dietrich A and Stolz W 1999 *J. Lumin.* **85** 45–58
Trautmann T, Krbetschek M R and Stolz W 2000 *Radiat. Meas.* **32** 685–90
Visocekas R and Zink A 1999 *Quat. Sci. Rev.* **18** 271–8